Effect of decay cascade via an intermediate resonance in the $\gamma p \to \pi^0 \eta p$ reaction*

Ai-Chao Wang (王爱超)[1] Neng-Chang Wei (韦能昌)[2†]

[1]College of Science, China University of Petroleum (East China), Qingdao 266580, China
[2]School of Physics, Henan Normal University, Xinxiang 453007, China

Abstract: The $\gamma p \to \pi^0 \eta p$ reaction has been investigated by the CBELSA/TAPS collaboration, revealing a narrow structure in the ηp invariant mass distributions at a mass of 1700 MeV. In this study, we explore the possibility of the narrow structure being caused by a decay cascade via an intermediate nucleon resonance decaying to ηp final states. The candidates for the intermediate nucleon resonances are $N(1700)3/2^-$ and $N(1710)1/2^+$, with masses near the observed structure. We considered the t-channel ρ- and ω-exchange diagrams, u-channel nucleon-pole exchange diagram, contact term, and s-channel pole diagrams of the nucleon, Δ, along with the nucleon resonances when constructing the reaction amplitudes, to reproduce the stripped individual contribution of the narrow structure. Our analysis indicates that the signature strength of the decay cascade $\gamma p \to \pi^0 N(1700)3/2^- \to \pi^0 \eta p$ is too weak to reach the experimental curve of the narrow structure due to the small decay branching ratio of $N(1700)3/2^-$ to ηp. Although the decay cascade $\gamma p \to \pi^0 N(1710)1/2^+ \to \pi^0 \eta p$ can qualitatively reproduce the experimental curve of the invariant mass distributions, its cross-section width is much larger than that of the corresponding experimental curve. Therefore, we conclude that the decay cascade via an intermediate nucleon resonance cannot be the reason for the narrow structure in the ηp invariant mass distributions of the $\gamma p \to \pi^0 \eta p$ reaction.

Keywords: nucleon resonance, photoproduction, decay cascade

DOI: 10.1088/1674-1137/add09f **CSTR:** 32044.14.ChinesePhysicsC.49083109

I. INTRODUCTION

The exploration of the structure and spectrum of nucleon resonances (N^*'s) and Δ resonances (Δ^*'s) has been a focal point in the field of hadron physics. This line of investigation offers valuable insights into the dynamic properties of quantum chromodynamics (QCD) in the nonperturbative energy regime. Our current understanding of nucleon resonances primarily stems from studies involving πN scattering and π photoproduction reactions. However, a substantial number of theoretically predicted nucleon resonances, originating from QCD-inspired phenomenological models [1−3] and QCD-lattice calculations [4, 5], have eluded experimental identification. This discrepancy is particularly evident in the center-of-mass energy (c.m.) 2 GeV region, where the observed nucleon resonances tend to be broader and more susceptible to overlapping. The number of theoretically predicted nucleon resonances surpasses the number of experimentally observed ones, leading to the so-called *missing resonance problem* [6].

One possible explanation for not detecting the missing resonances experimentally is their weak couplings to the πN channel, making them challenging to observe in such a reaction channel. Thus, investigating the πN-weakly-coupled nucleon resonances through other meson production reactions becomes a viable approach. In recent decades, significant progress has been made in meson photoproduction, both theoretically and experimentally, providing alternative platforms for nucleon resonance studies [7−23]. In this work, we employed the effective Lagrangian method to explore the potential impact of the decay cascade via intermediate nucleon resonance in the $\gamma p \to \pi^0 \eta p$ reaction. As a double-meson emission reaction, the $\gamma p \to \pi^0 \eta p$ reaction has a higher threshold energy than most single-meson emission reactions, making it more suitable for investigating high-mass nucleon resonances in the less-explored energy region.

Received 25 February 2025; Accepted 24 April 2025; Published online 25 April 2025

* Partially supported by the National Natural Science Foundation of China (12305097, 12305137), the Fundamental Research Funds for the Central Universities (23CX06037A), the Shandong Provincial Natural Science Foundation, China (ZR2024QA096), and the Taishan Scholar Young Talent Program (tsqn202408091)

† E-mail: E-mail: weinengchang@htu.edu.cn

Several experimental and theoretical studies have been conducted to investigate the $\gamma p \to \pi^0\eta p$ reaction [24−29] and provide a foundational understanding of its reaction mechanism. In [24], the $\gamma p \to \pi^0\eta p$ and $\gamma p \to \pi^0 K^0\Sigma^+$ reactions were analyzed using a chiral unitary approach. They showed that the contribution from the $\Delta(1700)3/2^-$ resonance, followed by its decay into $\Delta(1232)\eta$, plays a dominant role in the $\gamma p \to \pi^0\eta p$ reaction, establishing the basic mechanism of this process. The analysis in [25] also emphasized the importance of the $\Delta(1700)3/2^-$ resonance decaying into $\Delta(1232)\eta$, as a key contributor to the reaction. In [26], measurements of the total and differential cross sections are presented for the $\gamma p \to \pi^0\eta p$ reaction, revealing that in the energy range $E_\gamma = 0.95 - 1.4$ GeV, the reaction is predominantly driven by the excitation and sequential decay of the $\Delta(1700)3/2^-$ resonance. In [27], the partial wave structure of the $\gamma p \to \pi^0\eta p$ reaction was analyzed over a total center-of-mass energy range from threshold up to $W = 1.9$ GeV. The analysis indicated that the partial wave with quantum numbers $J^P = 3/2^-$ accounts for the largest fraction of the cross section, predominantly saturated by the $\Delta(1700)3/2^-$ resonance. In [28] a chiral unitary framework was employed to evaluate the polarization observables I^S and I^C for the $\gamma p \to \pi^0\eta p$ reaction, further corroborating the significant role of the $\Delta(1700)3/2^-$ resonance. In [29], beam-helicity asymmetry data were reported for the photoproduction of $\pi^0\eta$ pairs on carbon, aluminum, and lead, demonstrating that the $\gamma p \to \pi^0\eta p$ reaction is dominated by the D_{33} partial wave with the $\Delta(1232)\eta$ intermediate state. In summary, these studies consistently agree that the primary mechanism underlying the $\gamma p \to \pi^0\eta p$ reaction is dominated by the contribution from the $\Delta(1700)3/2^-$ resonance, decaying via $\Delta(1700) \to \Delta(1232)\eta$. Additionally, several other studies have contributed to the understanding of the $\gamma p \to \pi^0\eta p$ reaction [30−34].

Focusing on the present study, in 2017, a narrow structure was reported in the ηN invariant mass distribution at $W \sim 1.678$ GeV for the $\gamma N \to \pi\eta N$ reaction, based on data from the GRAAL facility [35]. The suggested interpretation was that the observed peak structure corresponds to the nucleon resonance $N(1685)$. Subsequently, in 2021, the CBELSA/TAPS collaboration conducted a remeasurement of the $\gamma p \to \pi^0\eta p$ reaction [36]. Contrary to the previous findings, they could not confirm the existence of a narrow structure in the ηN invariant mass distributions at $W \sim 1.678$ GeV. Instead, they observed a narrow structure in the ηp invariant mass distributions at $W \sim 1.7$ GeV, with a width of $\Gamma \approx 35$ MeV, for incident photon energies in the range of 1400−1500 MeV and a cut of $M_{\pi^0 p} \leq 1190$ MeV. Furthermore, with increasing incident energy from 1420 to 1540 MeV, the mass structure shifted from 1700 to 1725 MeV, and the width increased to about 50 MeV. The CBELSA/TAPS collaboration proposed that the most likely explanation for the narrow structure is a triangular singularity in the $\gamma p \to \pi^0\eta p$ reaction. Therefore, we were curious whether there were other possibilities that could explain the observed structure.

In this study, our objective was to investigate whether the observed narrow structure in the invariant mass distributions of the $\gamma p \to \pi^0\eta p$ reaction can be attributed to a decay cascade via an intermediate nucleon resonance into the ηp final states. While the dominant contribution of the decay cascade via the $\Delta(1232)$ resonance in this reaction is well established, we aimed to elucidate the role of other potential decay cascades involving nucleon resonances. Considering that the narrow structure is located at $M_{p\eta} = 1700\,\mathrm{MeV}/c^2$ and isospin conservation restricts the intermediate resonance to an isospin-1/2 nucleon resonance, we focused on two candidates in close proximity to this mass: $N(1700)3/2^-$, a three-star nucleon resonance in the Particle Data Group (PDG) review [37], and $N(1710)1/2^+$, a four-star nucleon resonance.

The CBELSA/TAPS collaboration has extracted the individual contributions to the narrow structure from the $\gamma p \to \pi^0\eta p$ reaction [36]. In this study, we aimed to reproduce this extracted narrow structure signal by employing the effective Lagrangian method and considering the decay cascade via possible intermediate resonances. Specifically, to construct the reaction amplitudes for the decay cascade $\gamma p \to \pi^0 Res.(\eta p) \to \pi^0\eta p$, we included contributions from the t-channel ρ- and ω-exchange, s-channel nucleon (N) and Δ pole diagrams, u-channel nucleon (N) pole exchange, and the contact term. For the decay cascade $\gamma p \to \pi^0 N(1700)3/2^- \to \pi^0\eta p$, contributions from nucleon resonances $N(1440)1/2^+$ and $N(1520)3/2^-$ were included. Similarly, for the decay cascade $\gamma p \to \pi^0 N(1710)1/2^+ \to \pi^0\eta p$, the contribution from the nucleon resonance $N(1535)1/2^-$ was considered. Notably, our model specifically excludes the dominant background process $\gamma p \to \Delta(1232)\eta \to \pi^0\eta p$, as this mechanism is not part of the extracted narrow structure signal.

To focus on the narrow structure, we employed specific operations for the theoretical framework. Following the approach in [36], an invariant mass distribution cut of $M_{p\pi^0} < 1190$ MeV was applied to suppress the dominant decay cascade $\gamma p \to \Delta(1232)\eta \to \pi^0\eta p$, to ensure consistency with the experimental data. Although the contribution from the $\Delta(1700)3/2^-$ resonance, which decays via $\Delta(1700) \to \Delta(1232)\eta$, is inherently part of the background, it was excluded from our theoretical model as it does not contribute to the narrow structure. Instead, our goal was to reproduce the individual contribution of the narrow structure extracted by the CBELSA/TAPS collaboration [36]. As such, the interference effects between the narrow structure and background terms were beyond the scope of this study. This approach allowed us to investigate whether the decay cascade via an intermediate nucle-

on resonance, $\gamma p \to \pi^0 Res. \to \pi^0\eta p$, can explain the observed narrow structure in the ηp invariant mass distributions of the $\gamma p \to \pi^0\eta p$ reaction. The results were in accordance with the energy-dependent relationship identified by the CBELSA/TAPS collaboration.

The current paper is organized as follows. In Sec. II, we provide an introduction to the framework of our theoretical model, encompassing Lagrangians, propagators, form factors, and reaction amplitudes. In Sec. III, we present the theoretical results and further discuss them. Finally, Sec. IV offers a summary and conclusions.

II. FORMALISM

The full reaction amplitude for the decay cascade reaction $\gamma p \to \pi^0 Res. \to \pi^0\eta p$ can be expressed as follows:

$$M = \bar{u}(p_5, \lambda_{p'}) A_\mu M^\mu u(p_2, \lambda_p), \tag{1}$$

where λ_p and $\lambda_{p'}$ are the helicities of the incoming proton and outgoing proton, respectively; μ is the Lorentz index of the incoming photon; and M^μ is the full amplitude with outer lines omitted. As observed in Fig. 1, the contributions considered in constructing the reaction amplitudes include: i) s-channel N, Δ, and N^* pole diagrams, ii) t-channel ρ- and ω-exchange diagrams, iii) u-channel N-pole exchange diagram, and iv) contact term diagram. In the decay cascade $\gamma p \to \pi^0 N(1700)3/2^- \to \pi^0\eta p$, N^* denotes the nucleon resonances $N(1440)1/2^+$ and $N(1520)3/2^-$, one of which, together with π, constitutes

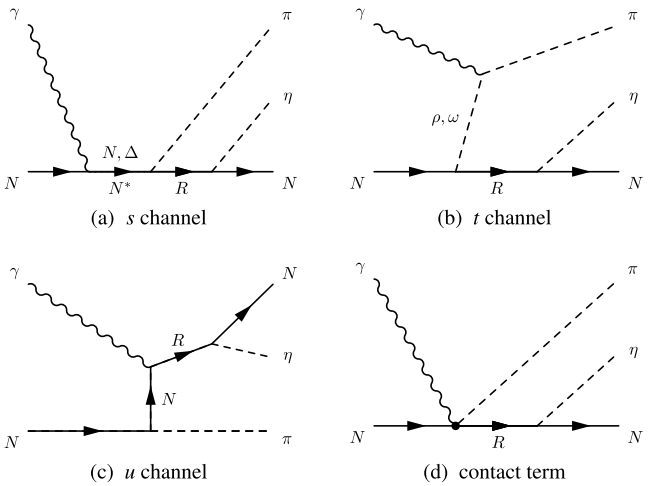

Fig. 1. Generic structure of the amplitudes for the decay cascade $\gamma N \to \pi Res. \to \pi\eta N$ reaction. For the case of $\gamma p \to \pi^0 N(1700)3/2^- \to \pi^0\eta p$ reaction, the R represents the intermediate resonance $N(1700)3/2^-$, and N^* represents the $N(1440)1/2^+$ and $N(1520)3/2^-$ resonances. For the case of $\gamma p \to \pi^0 N(1710)1/2^+ \to \pi^0\eta p$ reaction, the R represents the intermediate resonance $N(1710)1/2^+$, and N^* represents the $N(1535)1/2^-$ resonance. Time proceeds from left to right.

the decay mode of $N(1700)3/2^-$ as presented in the PDG review [37]. Similarly, for the decay cascade $\gamma p \to \pi^0 N(1710)1/2^+ \to \pi^0\eta p$, N^* represents the nucleon resonance $N(1535)1/2^-$.

In the remainder of this section, we present the effective Lagrangians, propagators, and phenomenological form factors used in this work to construct the reaction amplitudes. Additionally, we outline the final forms of the reaction amplitudes for all the particle-exchange cases in the two cascade decay reactions.

A. Effective Lagrangians

The effective Lagrangians utilized in our present work are provided below. For convenience, we define the field-strength tensor for the electromagnetic and vector-meson fields as

$$F^{\mu\nu} = \partial^\mu A^\nu - \partial^\nu A^\mu, \quad V^{\mu\nu} = \partial^\mu V^\nu - \partial^\nu V^\mu, \tag{2}$$

where V represents the ρ or ω vector meson.

1. *The effective Lagrangians for the electromagnetic vertices in the $\gamma N \to \pi N(1700)3/2^- \to \pi\eta N$ process*

$$\mathcal{L}_{NN\gamma} = -e\bar{N}\left[\left(\hat{e}\gamma^\mu - \frac{\hat{\kappa}_N}{2M_N}\sigma^{\mu\nu}\partial_\nu\right)A_\mu\right]N, \tag{3}$$

$$\mathcal{L}_{\pi\rho\gamma} = e\frac{g_{\pi\rho\gamma}}{M_\pi}\varepsilon^{\alpha\mu\lambda\nu}(\partial_\alpha A_\mu)(\partial_\lambda\pi)\rho_\nu, \tag{4}$$

$$\mathcal{L}_{\pi\omega\gamma} = e\frac{g_{\pi\omega\gamma}}{M_\pi}\varepsilon^{\alpha\mu\lambda\nu}(\partial_\alpha A_\mu)(\partial_\lambda\pi^0)\omega_\nu, \tag{5}$$

$$\begin{aligned}\mathcal{L}_{\Delta N\gamma} = &-\mathrm{i}e\frac{g^{(1)}_{\Delta N\gamma}}{2M_N}\bar{\Delta}_\mu\gamma_\nu\gamma_5 F^{\mu\nu}N \\ &+ e\frac{g^{(2)}_{\Delta N\gamma}}{(2M_N)^2}\bar{\Delta}_\mu\gamma_5 F^{\mu\nu}\partial_\nu N + \mathrm{H.c.},\end{aligned} \tag{6}$$

$$\begin{aligned}\mathcal{L}_{RN\gamma} = &-\mathrm{i}e\frac{g^{(1)}_{RN\gamma}}{2M_N}\bar{R}_\mu\gamma_\nu F^{\mu\nu}N \\ &+ e\frac{g^{(2)}_{RN\gamma}}{(2M_N)^2}\bar{R}_\mu F^{\mu\nu}\partial_\nu N + \mathrm{H.c.},\end{aligned} \tag{7}$$

$$\mathcal{L}_{RN\pi\gamma} = -\mathrm{i}e\frac{g_{RN\pi}}{M_\pi}\bar{R}^\mu\gamma_5 A_\mu\pi N + \mathrm{H.c.}, \tag{8}$$

$$\mathcal{L}^{1/2^+}_{N^*N\gamma} = e\frac{g^{(1)}_{N^*N\gamma}}{2M_N}\bar{N}^*\sigma^{\mu\nu}(\partial_\nu A_\mu)N + \mathrm{H.c.}, \tag{9}$$

$$\mathcal{L}^{3/2^-}_{N^*N\gamma} = -\mathrm{i}e\frac{g^{(1)}_{N^*N\gamma}}{2M_N}\bar{N}^*_\mu\gamma_\nu F^{\mu\nu}N + e\frac{g^{(2)}_{N^*N\gamma}}{(2M_N)^2}\bar{N}^*_\mu F^{\mu\nu}\partial_\nu N + \mathrm{H.c.}, \tag{10}$$

where e is the elementary charge unit; $\hat{e}$ and R represent the charge operator and nucleon resonance $N(1700)3/2^-$, respectively; The anomalous magnetic moments are defined as $\hat{\kappa}_N = \kappa_p(1+\tau_3)/2 + \kappa_n(1-\tau_3)/2$, where $\kappa_p = 1.793$ and $\kappa_n = -1.913$. M_N stands for the mass of N. The coupling constants $g_{\pi\rho\gamma}$ and $g_{\pi\omega\gamma}$ are determined by calculating the vector meson radiative decay width

$$\Gamma_{V\to\pi\gamma} = \frac{e^2}{4\pi}\frac{g^2_{V\pi\gamma}}{24M_V^3M_\pi^2}(M_V^2 - M_\pi^2)^3, \tag{11}$$

where V stands for the vector meson ρ or ω. Utilizing the decay width values $\Gamma_{\rho^0\to\pi^0\gamma} \simeq 0.070$ MeV and $\Gamma_{\omega\to\pi^0\gamma} \simeq 0.72$ MeV from the PDG review [37], we obtain $g_{\pi\rho\gamma} = 0.099$ and $g_{\pi\omega\gamma} = 0.31$. The coupling constants for $RN\gamma$ are determined by the PDG values of $N(1700)3/2^- \to N\gamma$ helicity amplitudes: $A_{1/2} = 0.032\ \mathrm{GeV}^{-1/2}$ and $A_{3/2} = 0.034\ \mathrm{GeV}^{-1/2}$, yielding $g^{(1)}_{RN\gamma} = 0.405$ and $g^{(2)}_{RN\gamma} = -0.986$. Similarly, $\Delta N\gamma$ couplings are determined by the PDG values of $\Delta(1232)3/2^+ \to N\gamma$ helicity amplitudes: $A_{1/2} = -0.135\ \mathrm{GeV}^{-1/2}$ and $A_{3/2} = -0.255\ \mathrm{GeV}^{-1/2}$, leading to $g^{(1)}_{\Delta N\gamma} = -4.17$ and $g^{(2)}_{\Delta N\gamma} = 4.32$. The s-channel $N(1440)1/2^+$ and $N(1520)3/2^-$ pole diagrams were considered due to their coupling with $\pi N(1700)3/2^-$ as stated in the PDG review [37]. The coupling constant of $N(1440)1/2^+N\gamma$ vertex was taken as $g^{(1)}_{N^*N\gamma} = 0.505$, obtained from the helicity amplitude $A_{1/2} = -0.065\ \mathrm{GeV}^{-1/2}$. The coupling constants of the $N(1520)3/2^-N\gamma$ vertex were taken as $g^{(1)}_{N^*N\gamma} = -4.86$ and $g^{(2)}_{N^*N\gamma} = 5.27$, derived from the helicity amplitudes $A_{1/2} = -0.025\ \mathrm{GeV}^{-1/2}$ and $A_{3/2} = 0.14\ \mathrm{GeV}^{-1/2}$ [37].

It is important to note that in the present work, the couplings of $N^*N\gamma$ were determined from the helicity amplitudes using the following relations, with all helicity amplitudes taken from the PDG review [37].

For a spin-1/2 resonance with parity $P = \pm 1$, the relation is given by

$$\bar{g}_1 = -\frac{1}{e}\sqrt{\frac{M_N}{kM_{N^*}}}A_{1/2}, \tag{12}$$

where

$$\bar{g}_1 = \frac{g^{(1)}_{N^*Nr}}{2M_N}. \tag{13}$$

For a spin-3/2 resonance with parity $P = \pm 1$, the relations are

$$\bar{g}_1 = \frac{1}{e}\frac{1}{\sqrt{2}k}\sqrt{\frac{M_N}{kM_{N^*}}}\left[\sqrt{3}A_{1/2} \pm A_{3/2}\right](M_{N^*} \mp M_N), \tag{14}$$

$$\bar{g}_2 = -\frac{1}{e}\frac{\sqrt{2}}{kM_{N^*}}\sqrt{\frac{M_N}{kM_{N^*}}}\left[\sqrt{3}M_{N^*}A_{1/2} - M_NA_{3/2}\right], \tag{15}$$

where

$$\bar{g}_1 = \frac{g^{(1)}_{N^*Nr}}{2M_N}, \qquad \bar{g}_2 = \frac{g^{(2)}_{N^*Nr}}{(2M_N)^2}. \tag{16}$$

2. *The effective Lagrangians for the electromagnetic vertices in the $\gamma N \to \pi N(1710)1/2^+ \to \pi\eta N$ process*

The Lagrangians outlined in Eqs. (3)−(6) are also required for constructing the amplitudes in the $\gamma N \to \pi N(1710)1/2^+$ reaction. The additional Lagrangians that are required are presented below:

$$\mathcal{L}_{RN\gamma} = e\frac{g^{(1)}_{RN\gamma}}{2M_N}\bar{R}\sigma^{\mu\nu}(\partial_\nu A_\mu)N + \mathrm{H.c.}, \tag{17}$$

$$\mathcal{L}_{RN\pi\gamma} = \mathrm{i}e\frac{g_{RN\pi}}{M_N + M_R}\bar{R}\gamma_5\gamma^\mu A_\mu\pi N + \mathrm{H.c.}, \tag{18}$$

$$\mathcal{L}^{1/2^-}_{N^*N\gamma} = e\frac{g^{(1)}_{N^*N\gamma}}{2M_N}\bar{N}^*\gamma_5\sigma^{\mu\nu}(\partial_\nu A_\mu)N + \mathrm{H.c.}, \tag{19}$$

where R represents the nucleon resonance $N(1710)1/2^+$. Additionally, the s-channel $N(1535)1/2^-$ pole diagram was considered because of its coupling with $\pi N(1710)1/2^+$, as stated in the PDG review [37]. The coupling constants for $N(1710)1/2^+N\gamma$ and $N(1535)1/2^-N\gamma$ vertices were estimated as $g^{(1)}_{RN\gamma} = 0.134$ and $g^{(1)}_{N^*N\gamma} = 0.619$ based on their respecctive decay branching widths $\Gamma_{N(1710)1/2^+\to N\gamma} \simeq 80\times 0.04\% = 0.032$ MeV and $\Gamma_{N(1535)1/2^+\to N\gamma} \simeq 150\times 0.23\% = 0.345$ MeV.

To reconcile the observed narrow structure width of approximately 35−50 MeV with the relatively broader PDG-reported widths of the candidate resonances $N(1700)3/2^-$ and $N(1710)1/2^+$, we assumed a total width of 80 MeV for both resonances in our analysis. The PDG-reported total widths, ranging from 100 to 300 MeV for $N(1700)3/2^-$ and from 80 to 200 MeV for $N(1710)1/2^+$, were derived from a comprehensive set of photo- and hadroproduction data. Whether the assumed values in our study are consistent with the full dataset from which the PDG widths were determined remains an open question. It should be emphasized that the observed narrow structure in the ηp invariant mass spectrum, with a width of approximately 35−50 MeV, arises from the interference effects among the relevant reaction amplitudes rather than

directly reflecting the intrinsic widths of the contributing resonances.

The width formula for the nucleon resonance with spin 1/2 decaying into $N\gamma$ is denoted as

$$\Gamma^{1/2\pm}_{N^*\to N\gamma} = \frac{e^2}{4\pi}\frac{g^{(1)^2}_{N^*N\gamma}}{(2M_N)^2}4k^3, \tag{20}$$

which is applicable to both nucleon resonances $N(1710)1/2^+$ and $N(1535)1/2^-$.

3. *The effective Lagrangians for meson-baryon vertexes in the $\gamma N \to \pi N(1700)3/2^- \to \pi\eta N$ process*

$$\mathcal{L}_{RN\pi} = \frac{g_{RN\pi}}{M_\pi}\bar{R}^\mu\gamma_5\left(\partial_\mu\pi\right)N + \text{H.c.}, \tag{21}$$

$$\mathcal{L}_{RN\eta} = -\frac{g_{RN\eta}}{M_\eta}\bar{N}\gamma_5\left(\partial_\mu\eta\right)R^\mu + \text{H.c.}, \tag{22}$$

$$\begin{aligned}\mathcal{L}_{R\Delta\pi} = {}& \frac{g^{(1)}_{R\Delta\pi}}{M_\pi}\bar{\Delta}_\mu\gamma^\alpha(\partial_\alpha\pi)R^\mu \\ & + \mathrm{i}\frac{g^{(2)}_{R\Delta\pi}}{M^2_\pi}\bar{\Delta}_\alpha(\partial^\mu\partial^\alpha\pi)R_\mu + \text{H.c.},\end{aligned} \tag{23}$$

$$\begin{aligned}\mathcal{L}_{RN\rho} = {}& -\mathrm{i}\frac{g^{(1)}_{RN\rho}}{2M_N}\bar{R}_\mu\gamma_\nu\rho^{\mu\nu}N + \frac{g^{(2)}_{RN\rho}}{(2M_N)^2}\bar{R}_\mu\rho^{\mu\nu}\partial_\nu N \\ & + \frac{g^{(3)}_{RN\rho}}{(2M_N)^2}\bar{R}_\mu(\partial_\nu\rho^{\mu\nu})N + \text{H.c.},\end{aligned} \tag{24}$$

$$\begin{aligned}\mathcal{L}_{RN\omega} = {}& -\mathrm{i}\frac{g^{(1)}_{RN\omega}}{2M_N}\bar{R}_\mu\gamma_\nu\omega^{\mu\nu}N + \frac{g^{(2)}_{RN\omega}}{(2M_N)^2}\bar{R}_\mu\omega^{\mu\nu}\partial_\nu N \\ & + \frac{g^{(3)}_{RN\omega}}{(2M_N)^2}\bar{R}_\mu(\partial_\nu\omega^{\mu\nu})N + \text{H.c.},\end{aligned} \tag{25}$$

$$\mathcal{L}_{NN\pi} = -g_{NN\pi}\bar{N}\gamma_5\left[\left(\mathrm{i}\lambda + \frac{1-\lambda}{2M_N}\not{\partial}\right)\pi\right]N, \tag{26}$$

$$\mathcal{L}^{1/2^+}_{N^*R\pi} = \frac{g^{(1)}_{N^*R\pi}}{M_\pi}\bar{R}^\mu\gamma_5(\partial_\mu\pi)N^* + \text{H.c.}, \tag{27}$$

$$\begin{aligned}\mathcal{L}^{3/2^-}_{N^*R\pi} = {}& \frac{g^{(1)}_{N^*R\pi}}{M_\pi}\bar{R}^\mu\gamma^\alpha\gamma_5(\partial_\alpha\pi)N^*_\mu \\ & + \mathrm{i}\frac{g^{(2)}_{N^*R\pi}}{M^2_\pi}\bar{R}_\alpha\gamma_5(\partial^\mu\partial^\alpha\pi)R_\mu + \text{H.c.},\end{aligned} \tag{28}$$

where the R represents the nucleon resonance $N(1700)3/2^-$. The coupling constants $g_{RN\pi}$, $g_{RN\eta}$, and $g^{(1)}_{R\Delta\pi}$ can be determined by the branching width of $N(1700)3/2^-$ decaying to $N\pi$, $N\eta$, and $\Delta\pi$, respectively. The width formulas are expressed as follows:

$$\Gamma_{R\to NP} = \frac{g^2_{RNP}}{4\pi}\frac{1}{3}\frac{k^3}{M_R M^2_P}(E_N - M_N), \tag{29}$$

$$\begin{aligned}\Gamma_{R\to\Delta\pi} = {}& \frac{1}{36\pi}\frac{k}{M_R M^2_\Delta}(E_\Delta + M_\Delta) \\ & \times\left\{\frac{g^{(1)^2}_{R\Delta\pi}}{M^2_\pi}(M_R - M_\Delta)^2\right. \\ & \times\left(2E^2_\Delta + 2E_\Delta M_\Delta + 5M^2_\Delta\right) \\ & + 2\frac{g^{(1)}_{R\Delta\pi}g^{(2)}_{R\Delta\pi}}{M^3_\pi}M_R k^2(M_R - M_\Delta)(2E_\Delta + M_\Delta) \\ & \left. + 2\frac{g^{(2)^2}_{R\Delta\pi}}{M^4_\pi}M^2_R k^4\right\},\end{aligned} \tag{30}$$

where P represents the pseudoscalar meson π or η. In the present study, the total decay width of $N(1700)3/2^-$ was assumed to be 80 MeV. Accordingly, the coupling constants for the $RN\pi$, $RN\eta$, and $R\Delta\pi$ vertices were estimated as $g_{RN\pi} = 0.588$, $g_{RN\eta} = 2.08$, and $g^{(1)}_{R\Delta\pi} = -0.386$ based on the decay branching widths $\Gamma_{R\to N\pi} \simeq 80\times 12\% = 9.6$ MeV, $\Gamma_{R\to N\eta} \simeq 80\times 1.5\% = 1.2$ MeV, and $\Gamma_{R\to\Delta\pi} \simeq 80\times 70\% = 56$ MeV. These branching ratios are referenced from the PDG review [37]. For simplicity, we omit the $g^{(2)}$ and $g^{(3)}$ terms in the Lagrangians of $R\Delta\pi$, $RN\rho$, $RN\omega$, and $N^*R\pi$ couplings due to lack of experimental information. Consequently, the energy-dependent width formula for RNV coupling can be expressed as

$$\begin{aligned}\Gamma_{R\to NV}(\sqrt{s}) = {}& \frac{1}{12\pi}\frac{k}{M_R}(E_N + M_N) \\ & \times\frac{g^{(1)^2}_{RNV}}{4M^2_N}\left[2E_N(E_N - M_N) + (M_R - M_N)^2 + 2M^2_V\right],\end{aligned} \tag{31}$$

where V represents the vector meson ρ or ω. Additionally, for the decay process $R\to\rho N/\omega N$, considering that the mass of the nucleon resonance $N(1700)3/2^-$ lies close to the $\rho N/\omega N$ threshold, the effect of finite decay width has to be accounted for. Referring to previous studies [38–40], the final formula for the decay width of RNV is given by

$$\begin{aligned}\Gamma_{R\to NV} = {}& -\frac{1}{\pi}\int_{(M_R-2\Gamma_R)^2}^{(M_R+2\Gamma_R)^2}\Gamma_{R\to NV}(\sqrt{s}) \\ & \times\Theta(\sqrt{s} - M_N - M_V) \\ & \times\mathrm{Im}\left\{\frac{1}{s - M^2_R + \mathrm{i}M_R\Gamma_R}\right\}\mathrm{d}s.\end{aligned} \tag{32}$$

The coupling constants $g_{RN\rho} = 5.57$ and $g_{RN\omega} = 4.89$ were determined using the formulas above, along with the

estimated branching widths $\Gamma_{R\to N\rho}\simeq 80\times 38\%=30.4$ MeV and $\Gamma_{R\to N\omega}\simeq 80\times 22\%=17.6$ MeV. It is important to note that all the decay branching ratios in this work adopt the middle values within the suggested intervals by the PDG review [37]. Following [41], a pure pseudovector coupling ($\lambda=0$) was assumed for the $NN\pi$ vertex, with the coupling constant $g_{NN\pi}=0.989$ adopted from [42], as determined by the $SU(3)$ flavor symmetry. Additionally, the coupling constants for $N(1440)1/2^+R\pi$ and $N(1520)3/2^-R\pi$ were considered. The coupling constant $g^{(1)}_{N^*R\pi}$ for $N(1440)1/2^+R\pi$ was assumed to be 7.23 based on the decay branching width $\Gamma_{R\to N(1440)1/2^+\pi}\simeq 80\times 7\%=5.6$ MeV. Similarly, for $N(1520)3/2^-R\pi$, the coupling constant $g^{(1)}_{N^*R\pi}$ was calculated as -0.759, derived from the decay branching width $\Gamma_{R\to N(1535)1/2^-\pi}\simeq 80\times 4\%=3.2$ MeV. The width formulas are expressed as follows

$$\Gamma_{R\to N(1440)1/2^+\pi}=\frac{g^{(1)^2}_{N^*R\pi}}{4\pi}\frac{1}{3}\frac{k^3}{M_R M_\pi^2}(E_{N^*}-M_{N^*}), \tag{33}$$

$$\begin{aligned}\Gamma_{R\to N(1520)3/2^-\pi}=&\frac{1}{36\pi}\frac{k}{M_R M_{N^*}^2}(E_{N^*}-M_{N^*})\\&\times\left\{\frac{g^{(1)^2}_{N^*R\pi}}{M_\pi^2}(M_R+M_{N^*})^2\right.\\&\times\left(2E_{N^*}^2-2E_{N^*}M_{N^*}+5M_{N^*}^2\right)\\&+2\frac{g^{(1)}_{N^*R\pi}g^{(2)}_{N^*R\pi}}{M_\pi^3}M_R k^2(M_R+M_{N^*})\\&\left.\times(2E_{N^*}-M_{N^*})+2\frac{g^{(2)^2}_{N^*R\pi}}{M_\pi^4}M_R^2k^4\right\}.\end{aligned} \tag{34}$$

4. *The effective Lagrangians for meson-baryon vertexes in the $\gamma N\to\pi N(1710)1/2^+\to\pi\eta N$ process*

$$\mathcal{L}_{RN\pi}=-g_{RN\pi}\bar{R}\gamma_5\left[\left(\mathrm{i}\lambda+\frac{1-\lambda}{M_N+M_R}\partial\!\!\!/\right)\pi\right]N+\mathrm{H.c.}, \tag{35}$$

$$\mathcal{L}_{RN\eta}=-g_{RN\eta}\bar{R}\gamma_5\left[\left(\mathrm{i}\lambda+\frac{1-\lambda}{M_N+M_R}\partial\!\!\!/\right)\eta\right]N+\mathrm{H.c.}, \tag{36}$$

$$\mathcal{L}_{R\Delta\pi}=\frac{g^{(1)}_{R\Delta\pi}}{M_\pi}\bar{R}(\partial^\nu\pi)\Delta_\nu+\mathrm{H.c.}, \tag{37}$$

$$\mathcal{L}_{RN\rho}=-\frac{g_{RN\rho}}{2M_N}\bar{R}\left[\left(\frac{\gamma_\mu\partial^2}{M_R-M_N}+\mathrm{i}\partial_\mu\right)V^\mu\right]N+\mathrm{H.c.}, \tag{38}$$

$$\mathcal{L}_{RN\omega}=-\frac{g_{RN\omega}}{2M_N}\bar{R}\left[\left(\frac{\gamma_\mu\partial^2}{M_R-M_N}+\mathrm{i}\partial_\mu\right)V^\mu\right]N+\mathrm{H.c.}, \tag{39}$$

$$\mathcal{L}^{1/2^-}_{N^*R\pi}=-g^{(1)}_{N^*R\pi}\bar{R}\left[\left(\mathrm{i}\lambda+\frac{1-\lambda}{M_{N^*}-M_R}\partial\!\!\!/\right)\pi\right]N^*+\mathrm{H.c.}, \tag{40}$$

where the R denotes the nucleon resonance $N(1710)1/2^+$. Pure pseudovector-type couplings are employed for the $RN\pi$ and $RN\eta$ vertices. The coupling constants $g_{RN\pi}$, $g_{RN\eta}$, and $g^{(1)}_{R\Delta\pi}$ are determined through the branching width of $N(1710)1/2^+$ decaying into $N\pi$, $N\eta$, and $\Delta\pi$, respectively. The width formulas are expressed as follows:

$$\Gamma_{R\to NP}=\frac{g^2_{RNP}}{4\pi}\frac{k}{M_R}(E_N-M_N), \tag{41}$$

$$\Gamma_{R\to\Delta\pi}=\frac{g^{(1)^2}_{R\Delta\pi}}{6\pi}\frac{k^3M_R}{M_\pi^2M_\Delta^2}(E_\Delta+M_\Delta), \tag{42}$$

where P denotes the pseudoscalar meson π or η. The coupling constants for $RN\pi$, $RN\eta$, and $R\Delta\pi$ vertices are specified as $g_{RN\pi}=1.47$, $g_{RN\eta}=3.81$, and $g^{(1)}_{R\Delta\pi}=0.0973$ based on the decay branching widths $\Gamma_{R\to N\pi}\simeq 80\times 12.5\%=10$ MeV, $\Gamma_{R\to N\eta}\simeq 80\times 30\%=24$ MeV, and $\Gamma_{R\to\Delta\pi}\simeq 80\times 6\%=4.8$ MeV. The reaction energy-dependent width formula for the RNV coupling is simplified to

$$\begin{aligned}\Gamma_{R\to NV}(\sqrt{s})=&\frac{g^{(1)^2}_{RNV}}{16\pi}\frac{k(E_N-M_N)}{M_RM_N^2}\\&\times\left\{\frac{M_V^2}{(M_R-M_N)^2}\left[(M_R+M_N)^2+2M_V^2\right]\right\},\end{aligned} \tag{43}$$

where V represents the vector meson ρ or ω. Considering the effect of finite decaying width is essential [38–40], and the decay width formula remains consistent with Eq. (32). Consequently, the coupling constants $g_{RN\rho}=8.47$ and $g_{RN\omega}=4.16$ are obtained from the estimated branching widths $\Gamma_{R\to N\rho}\simeq 80\times 17\%=13.6$ MeV and $\Gamma_{R\to N\omega}\simeq 80\times 3\%=2.4$ MeV, respectively. A pure pseudovector-type coupling is also applied to the $N(1440)1/2^+R\pi$ vertex. The coupling constant for the $N(1535)1/2^-R\pi$ vertex is set as $g^{(1)}_{N^*R\pi}=0.864$, derived from the decay branching width $\Gamma_{R\to N(1535)1/2^-\pi}\simeq 80\times 15\%=12$ MeV. The width formula is expressed as

$$\Gamma_{R\to N(1535)1/2^-\pi}=\frac{g^{(1)^2}_{N^*R\pi}}{4\pi}\frac{k}{M_R}(E_N+M_N). \tag{44}$$

B. Propagators

For the s- and u-channel N, the propagator is represented as

$$S_{1/2}(p) = \frac{\mathrm{i}}{\not{p} - M_N}. \tag{45}$$

For the s-channel spin-1/2 resonance $N(1440)1/2^+$ and $N(1535)1/2^-$, the propagator is denoted as

$$S_{1/2}(p) = \frac{\mathrm{i}}{\not{p} - M_R + \mathrm{i}\Gamma_R/2}, \tag{46}$$

where M_R and Γ_R represent the mass and width of the resonance, respectively.

For the t-channel ρ or ω vector meson exchange, the propagator is denoted as

$$S_1(p) = \frac{\mathrm{i}(-g^{\mu\nu} + p^\mu p^\nu/M_V^2)}{p^2 - M_V^2}. \tag{47}$$

For the s-channel Δ contribution and subsequent decay process of the nucleon resonance $N(1700)3/2^-$, the propagator for a particle with spin 3/2 is given by

$$S_{3/2}(p) = \frac{\mathrm{i}}{\not{p} - M_R + \mathrm{i}\Gamma_R/2}\left(\tilde{g}_{\mu\nu} + \frac{1}{3}\tilde{\gamma}_\mu\tilde{\gamma}_\nu\right), \tag{48}$$

where

$$\tilde{g}_{\mu\nu} = -g_{\mu\nu} + \frac{p_\mu p_\nu}{M_R^2}, \tag{49}$$

$$\tilde{\gamma}_\mu = \gamma^\nu\tilde{g}_{\nu\mu} = -\gamma_\mu + \frac{p_\mu \not{p}}{M_R^2}. \tag{50}$$

C. Form factors

To parametrize the structure of the hadrons and normalize the behavior of the production amplitude, a form factor should be attached to each hadronic vertex. Although two hadronic vertices exist in each reaction amplitude, only one form factor is introduced here. Following [41, 43], for intermediate baryon exchange, the form factor is expressed as

$$f_{s(u)}\left(p^2\right) = \left(\frac{\Lambda_B^4}{\Lambda_B^4 + \left(p^2 - M_B^2\right)^2}\right)^2, \tag{51}$$

where p, M_B, and Λ_B denote the four-momentum, mass, and cutoff mass of the exchanged baryon B, respectively. The same cutoff mass is employed for the s- and u-channel N. The particle mass in the form factor of the contact term is set to the same value as that of N. For intermediate meson exchange, the form factor is expressed as

$$f_t\left(q^2\right) = \left(\frac{\Lambda_M^2 - M_M^2}{\Lambda_M^2 - q^2}\right)^2, \tag{52}$$

where q, M_M, and Λ_M represent the four-momentum, mass, and cutoff mass for the exchanged meson M, respectively. The same cutoff mass is taken for the t-channel ρ and ω exchanges.

D. Reaction amplitudes

With all the Lagrangians, propagators, and form factors introduced above, the standard amplitudes for the decay cascade $\gamma p \to \pi^0 N(1700)3/2^- \to \pi^0\eta p$ can be expressed as

$$M^\mu = T_\nu M^{\mu\nu}, \tag{53}$$

where T_ν represents the $N(1700)3/2^- \to \eta p$ decay. This part is the same for all individual amplitudes of t-, u-, s-channel, and contact term and expressed as

$$T_\nu = \frac{g_{RN\eta}}{m_\eta}\gamma_5 p_4^\beta S^{3/2}_{\beta\nu}(p_R). \tag{54}$$

and $M^{\mu\nu}$ represents the remaining parts of the leg-amputated amplitudes M^μ, which are represented as follows:

$$M^{\mu\nu}_{N(s)} = \mathrm{i}e\frac{g_{RN\pi}}{m_\pi}\gamma_5 p_3^\nu S^{1/2}(p_s) \times \left[\gamma^\mu + \frac{\mathrm{i}\kappa_N}{2m_N}\sigma^{\mu\alpha}p_{1\alpha}\right] f_s(p_s, m_N),, \tag{55}$$

$$M^{\mu\nu}_{N(u)} = -\mathrm{i}\frac{g_{NN\pi}}{2m_N}(p_1^\nu g^{\mu\alpha} - p_1^\alpha g^{\mu\nu}) \times \left[\frac{eg^{(1)}_{RN\gamma}}{2m_N}\gamma_\alpha + \frac{eg^{(2)}_{RN\gamma}}{(2m_N)^2}p_{u\alpha}\right] \times S^{1/2}(p_u)\gamma_5 \not{p}_3 f_u(p_u, m_N), \tag{56}$$

$$M^{\mu\nu}_{\Delta} = \mathrm{i}\frac{g_{R\Delta\pi}}{m_\pi}\not{p}_3 g^{\lambda\nu}S^{3/2}_{\lambda\delta}(p_s)(p_1^\delta g^{\mu\beta} - p_1^\beta g^{\mu\delta}) \times \left[\frac{eg^{(1)}_{\Delta N\gamma}}{2m_N}\gamma_\beta\gamma_5 + \frac{eg^{(2)}_{\Delta N\gamma}}{(2m_N)^2}\gamma_5 p_{2\beta}\right] f_s(p_s, m_\Delta), \tag{57}$$

$$M^{\mu\nu}_{N(1440)} = -e\frac{g^{(1)}_{N^*R\pi}g^{(1)}_{N^*N\gamma}}{2m_\pi m_N}\gamma_5 p_3^\nu S^{1/2}(p_s) \times \sigma^{\mu\alpha}p_{1\alpha}f_s(p_s, m_{N(1440)}), \tag{58}$$

$$M^{\mu\nu}_{N(1520)} = \mathrm{i}\frac{g^{(1)}_{N^*R\pi}}{m_\pi}\not{p}_3\gamma_5 g^{\lambda\nu}S^{3/2}_{\lambda\delta}(p_s)(p_1^\delta g^{\mu\beta} - p_1^\beta g^{\mu\delta}) \times\left[\frac{e g^{(1)}_{N^*N\gamma}}{2m_N}\gamma_\beta + \frac{e g^{(2)}_{N^*N\gamma}}{(2m_N)^2}p_{2\beta}\right] f_s(p_s, m_{N(1520)}), \tag{59}$$

$$M^{\mu\nu}_{\rho} = -e\frac{g_{RN\rho}g_{\pi\rho\gamma}}{2m_\pi m_N}\epsilon^{\alpha\mu\lambda\delta}p_{1\alpha}p_{3\lambda}S^1_{\delta\sigma}(p_t) \times\gamma_\beta(p_t^\nu g^{\sigma\beta} - p_t^\beta g^{\sigma\nu})f_t(p_t, m_\rho), \tag{60}$$

$$M^{\mu\nu}_{\omega} = -e\frac{g_{RN\omega}g_{\pi\omega\gamma}}{2m_\pi m_N}\epsilon^{\alpha\mu\lambda\delta}p_{1\alpha}p_{3\lambda}S^1_{\delta\sigma}(p_t) \times\gamma_\beta(p_t^\nu g^{\sigma\beta} - p_t^\beta g^{\sigma\nu})f_t(p_t, m_\omega), \tag{61}$$

$$M^{\mu\nu}_{c} = e\frac{g_{RN\pi}}{m_\pi}g^{\mu\nu}\gamma_5 f_s(p_s, m_N), \tag{62}$$

where $p_s = p_1 + p_2$, $p_t = p_3 - p_1$, and $p_u = p_2 - p_3$.

Similarly, the standard amplitudes for the decay cascade $\gamma p \to \pi^0 N(1710)1/2^+ \to \pi^0\eta p$ can be expressed as

$$M^\mu(L) = TM^\mu(R), \tag{63}$$

where the L and R in the parentheses denote left and right, respectively; T represents the $N(1710)1/2^+ \to \eta p$ decay, which is given by

$$T = -\mathrm{i}\frac{g_{RN\eta}}{m_R + m_N}\gamma_5\not{p}_4 S^{1/2}(p_R). \tag{64}$$

The $M^\mu(R)$ represent the remaining parts of the leg-amputated amplitudes $M^\mu(L)$, expressed as

$$M^\mu_{N(s)} = -\mathrm{i}e\frac{g_{RN\pi}}{m_N - m_R}\gamma_5\not{p}_3 S^{1/2}(p_s) \times\left(\gamma^\mu + \frac{\mathrm{i}\kappa_N}{2m_N}\sigma^{\mu\beta}p_{1\beta}\right) f_s(p_s, m_N), \tag{65}$$

$$M^\mu_{N(u)} = e\frac{g_{NN\pi}g_{RN\gamma}}{(2m_N)^2}\sigma^{\mu\alpha}p_{1\alpha}S^{1/2}(p_u) \times\gamma_5\not{p}_3 f_u(p_u, m_N), \tag{66}$$

$$M^\mu_{\Delta} = \mathrm{i}\frac{g_{R\Delta\pi}}{m_\pi}p_3^\alpha S^{3/2}_{\alpha\delta}(p_s)(p_1^\delta g^{\mu\beta} - p_1^\beta g^{\mu\delta}) \times\left[\frac{e g^{(1)}_{RN\gamma}}{2m_N}\gamma_\beta\gamma_5 + \frac{e g^{(2)}_{\Delta N\gamma}}{(2m_N)^2}\gamma_5 p_{2\beta}\right] f_s(p_s, m_\Delta), \tag{67}$$

$$M^\mu_{N(1535)} = e\frac{g^{(1)}_{N^*R\pi}g^{(1)}_{N^*N\gamma}}{2m_N(m_R - m_N)}\not{p}_3 S^{1/2}(p_s) \times\gamma_5\sigma^{\mu\alpha}p_{1\alpha}f_s(p_s, m_{N(1535)}), \tag{68}$$

$$M^\mu_{\rho} = e\frac{g_{RN\rho}g_{\pi\rho\gamma}}{2m_\pi m_N}\left[\frac{-\gamma^\beta p_t^2}{m_R - m_N} - p_t^\beta\right] S^1_{\beta\delta}(p_t) \times\epsilon^{\alpha\mu\lambda\delta}p_{1\alpha}p_{3\lambda}f_t(p_t, m_\rho), \tag{69}$$

$$M^\mu_{\omega} = e\frac{g_{RN\omega}g_{\pi\omega\gamma}}{2m_\pi m_N}\left[\frac{-\gamma^\beta p_t^2}{m_R - m_N} - p_t^\beta\right] S^1_{\beta\delta}(p_t) \times\epsilon^{\alpha\mu\lambda\delta}p_{1\alpha}p_{3\lambda}f_t(p_t, m_\omega), \tag{70}$$

$$M^\mu_{c} = \mathrm{i}e\frac{g_{RN\pi}}{m_N + m_R}\gamma_5\gamma^\mu f_s(p_s, m_N). \tag{71}$$

The total amplitude M is obtained by summing the individual amplitudes. Notably, the total amplitude M is not gauge invariant in its current form because of the form factors. Specifically, for the $\gamma p \to \pi^0 N(1710)1/2^+ \to \pi^0\eta p$ process, the pole contributions from s-channel N and u-channel N break gauge invariance. Similarly, for the $\gamma p \to \pi^0 N(1700)3/2^- \to \pi^0\eta p$ process, the s-channel N pole contribution also breaks gauge invariance. In our previous studies [41, 43], we employed a generalized gauge-invariant term following the approach outlined in [44, 45] to ensure gauge invariance of the amplitude. However, given the multiple approximations adopted in the present work, we focus on maintaining the simplicity of the formalism. As a result, instead of incorporating the generalized gauge-invariant term, a general contact term is introduced. It should be noted that unlike the generalized gauge-invariant term, the general contact term does not preserve the gauge invariance of the amplitude. This limitation is acceptable within the scope of the present study, given the emphasis on simplicity and practical approximations.

The theoretical results for differential cross-sections, total cross-sections, and invariant mass distributions can be calculated using the formula

$$\mathrm{d}\sigma = \frac{1}{4(2\pi)^5(p_1\cdot p_2)}\sum_{\lambda_\gamma\lambda_p\lambda_{p'}}|M|^2\frac{\mathrm{d}^3p_3}{2E_\pi}\frac{\mathrm{d}^3p_4}{2E_\eta}\frac{\mathrm{d}^3p_5}{2E_{p'}} \times\delta^4(p_1 + p_2 - p_3 - p_4 - p_5), \tag{72}$$

where λ_γ, λ_p and $\lambda_{p'}$ are the helicities of the photon, incoming proton, and outgoing proton, respectively; p_1, p_2, p_3, p_4, p_5 are the four-momenta of the photon, incoming proton, π, η, and outgoing proton, respectively.

III. RESULTS AND DISCUSSION

Following the discovery of the narrow structure in the ηN invariant mass distributions at $W \sim 1.68$ GeV for the $\gamma N \to \pi\eta N$ reaction at the GRAAL facility [35], the CBELSA/TAPS collaboration remeasured the $\gamma p \to \pi^0\eta p$ reaction and observed the narrow structure at a different energy $W \sim 1.7$ GeV [36]. Two contrasting explanations have been proposed for this narrow structure. The first interpretation [35] suggests that the narrow structure results from a new isospin 1/2 nucleon resonance, denoted as $N(1685)$. In contrast, the CBELSA/TAPS collaboration, in their 2021 study [36], argued that the narrow structure is more likely caused by the triangular singularity in the $\gamma p \to \pi^0\eta p$ reaction rather than the decay cascade via an intermediate resonance.

Clarifying the nature of this narrow structure requires distinguishing between the contribution of the narrow structure and the dominant background originating from the $\gamma p \to \Delta(1232)\eta \to p\pi^0\eta$ mechanism, as identified by the CBELSA/TAPS collaboration [36]. In their analysis, the narrow structure signal (represented by the red solid curve in Fig. 7 of [36]) was extracted from the background dominated by the $\Delta(1232)$ resonance (depicted by the blue dotted curve in Fig. 7 of [36]). Our present work focused exclusively on reproducing the extracted narrow structure contribution rather than the entire $M_{p\eta}$ invariant mass spectrum. By isolating the narrow structure, we aimed to provide a quantitative assessment of whether the observed structure can result from the decay cascade via an intermediate nucleon resonance. Additionally, we explored the possible roles of decay cascades involving other intermediate resonances, beyond the dominant $\Delta(1232)$.

At the energy where the narrow structure was detected, approximately $W \sim 1.7$ GeV, the PDG review [37] lists two potential nucleon resonances: the evaluated three-star $N(1700)3/2^-$ and four-star $N(1710)1/2^+$. Both resonances have non-zero decay branching ratios to the ηp channel. Specifically, according to the PDG review, the decay branching ratio to ηp is estimated to be 1%−2% for the $N(1700)3/2^-$ and 10%−50% for the $N(1710)1/2^+$. For this study, we adopted the medians of these estimated ranges. The masses of the nucleon resonances $N(1700)3/2^-$ and $N(1710)1/2^+$ were taken as 1700 MeV and 1710 MeV, respectively. Our model intentionally excludes contributions from the $\gamma p \to \Delta(1232)\eta \to p\pi^0\eta$ mechanism, as these contribute primarily to the background rather than to the narrow structure of interest.

Regarding the width values, the PDG provides estimated ranges of 100−300 MeV for the $N(1700)3/2^-$ and 80−200 MeV for the $N(1710)1/2^+$. However, in our present work, we opted for a width of 80 MeV for both nucleon resonances. This choice was motivated by the observed behavior of the narrow structure in the data from the CBELSA/TAPS collaboration [36]. As the incident energy increases from 1420 to 1540 MeV, the width of the observed structure grows from 35 to approximately 50 MeV and then decreases. The chosen value of 80 MeV strikes a balance between the advocated width values by the PDG and experimental observations, by considering the potential interference effects between the individual contribution of the narrow structure and its background.

To investigate whether the narrow structure in the ηp invariant mass distributions can be attributed to the decay cascade via the intermediate nucleon resonance decay into the ηp final states, we employed an effective Lagrangian method at the tree-level approximation. Our study considers all the relevant terms based on decay information from the PDG review [37]. In addition to the background terms, including t-channel ρ and ω exchanges, s-channel N and Δ pole contributions, u-channel N exchange, and the contact term, we included the pole contributions of s-channel nucleon resonances coupled to the $\pi Res.$ channel. According to the PDG review, for the case of $\gamma p \to \pi^0 N(1700)3/2^- \to \pi^0\eta p$, we considered the nucleon resonances $N(1440)1/2^+$ and $N(1520)3/2^-$ and for $\gamma p \to \pi^0 N(1710)1/2^+ \to \pi^0\eta p$, the nucleon resonance $N(1535)1/2^-$ in the s channel.

As detailed in Sec. II, all coupling parameters in our study were fixed using decay branching ratios or helicity amplitudes referenced from the PDG review [37], providing a rigorous foundation for constructing the theoretical framework. The cutoff masses were treated as fitting parameters and are summarized in Table 1. Table 1 reveals that the same cutoff mass value is used for the t-channel ρ and ω exchanges and another common cutoff mass value for the remaining terms.

The theoretical results for the invariant mass distributions of the $\gamma p \to \pi^0 N(1700)3/2^- \to \pi^0\eta p$ decay cascade reaction, corresponding to the parameters of Model I listed in the second column of Table 1, are presented in Fig. 2. The black solid lines represent the theoretical predictions for the narrow structure contribution, whereas the blue scattered symbols correspond to the experimentally extracted narrow structure signal, as provided by the CBELSA/TAPS collaboration [36]. Notably, the experimental data have been processed with a cut of $M_{p\pi^0} < 1190$ MeV to suppress the dominant background from the decay cascade via the $\Delta(1232)$ resonance, which

Table 1. Model parameters. The same value is taken for the cutoff mass of the t-channel ρ and ω exchanges, as well as for the cutoff mass of the other terms.

	Model I	Model II
$\Lambda_{\rho,\omega}$/MeV	2500	1550
Λ_{others}/MeV	2500	2500

dominates in the $\gamma p \to \pi^0\eta p$ reaction. Our theoretical calculations also incorporate this cut, ensuring consistency with the experimental conditions and focusing on reproducing the narrow structure contribution.

As depicted in Fig. 2, the theoretical results fall short of reaching the order of magnitude of the experimental data. In other words, the decay cascade via the intermediate nucleon resonance $N(1700)3/2^-$ cannot account for the narrow structure observed in the ηp invariant mass distributions. The primary reason for this discrepancy is the weak coupling of the nucleon resonance $N(1700)3/2^-$ to the ηp final states, with a decay branching ratio of 1%−2% as indicated by the PDG review [37]. This leads to theoretical results with an order of magnitude lower than that of the data.

The theoretical results for the invariant mass distributions of the $\gamma p \to \pi^0 N(1710)1/2^+ \to \pi^0\eta p$ decay cascade, corresponding to the parameters of Model II as listed in the third column of Table 1, are presented in Fig. 3. The decay cascade via the intermediate nucleon resonance $N(1710)1/2^+$ provides a qualitative description of the stripped experimental curve, as depicted in Fig. 3. However, there is room for improvement in the description. The fixed width of the nucleon resonance $N(1710)1/2^+$ is 80 MeV, which surpasses that of the observed structure represented as 35 MeV [36]. The interference effect between the contribution of the narrow structure and the background terms introduces imprecision to the stripped contribution of the narrow structure. Thus, the current descriptive quality of Model II for the invariant mass distributions, illustrated in Fig. 3, is considered acceptable.

Nevertheless, as shown in Fig. 4, with increasing incident energy, the cross section of the decay cascade $\gamma p \to \pi^0 N(1710)1/2^+ \to \pi^0\eta p$ deviates significantly from the CBELSA/TAPS data of the narrow structure [36]. The observed data exhibit a much smaller cross-section width, and this substantial deviation cannot be solely attributed to the interference effects between the narrow structure and its background terms, or the fixed width of 80 MeV. Consequently, we conclude that regardless of whether the intermediate nucleon resonance is $N(1700)3/2^-$ or $N(1710)1/2^+$, the decay cascade via the intermediate nucleon resonance cannot account for the narrow structure observed in the ηp invariant mass distributions.

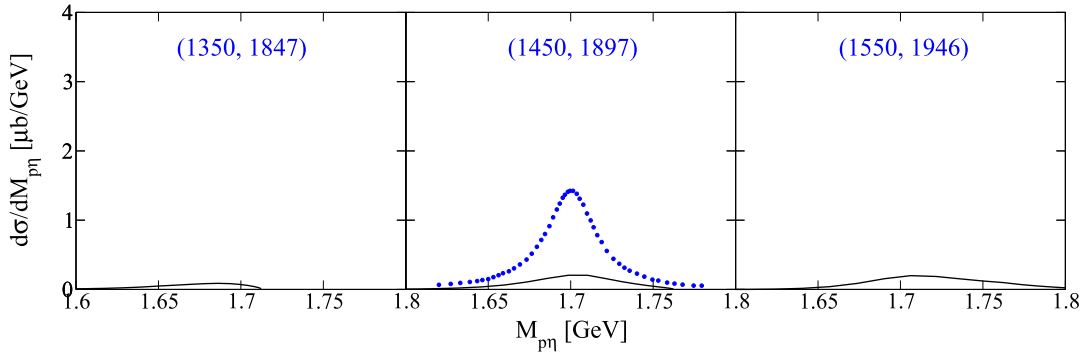

Fig. 2. (color online) The invariant mass distributions of decay cascade $\gamma p \to \pi^0 N(1700)3/2^- \to \pi^0\eta p$ as a function of the invariant mass of ηp (black solid lines). The blue scattered symbols denote the individual contribution of the narrow structure stripped by the CBELSA/TAPS collaboration [36]. The left number in parentheses denotes the centroid value of the photon laboratory incident energy and the right number corresponds to the total center-of-mass energy of the system in MeV.

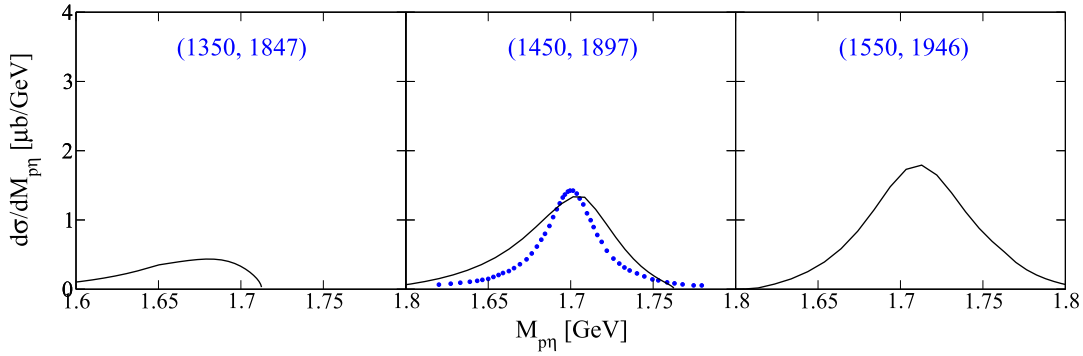

Fig. 3. (color online) The invariant mass distributions of decay cascade $\gamma p \to \pi^0 N(1710)1/2^+ \to \pi^0\eta p$ as a function of the invariant mass of ηp (black solid lines). The notation is the same as in Fig. 2.

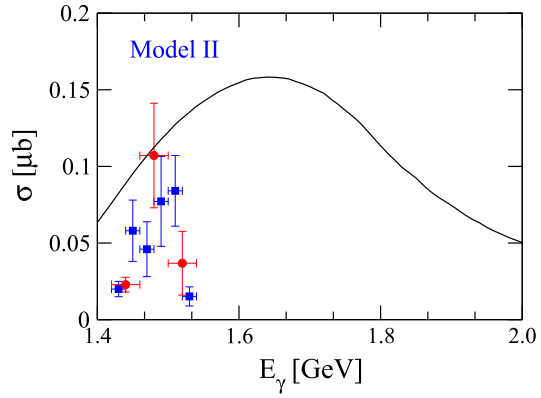

Fig. 4. (color online) The cross sections of the decay cascade $\gamma p \to \pi^0 N(1710)1/2^+ \to \pi^0\eta p$ as a function of the incident photon energy (black solid line). The blue and red scattered symbols correspond to the individual contributions of the narrow structure extracted by the CBELSA/TAPS collaboration [36].

IV. SUMMARY AND CONCLUSION

The CBELSA/TAPS collaboration detected a narrow structure in the ηp invariant mass distributions of the $\gamma p \to \pi^0\eta p$ reaction at an incident energy of $W \sim 1.7$ GeV [36]. Two distinct explanations have been proposed: the structure is attributed either to a new isospin-1/2 nucleon resonance $N(1685)$ [35] or to the triangular singularity mechanism [36]. Motivated by these interpretations, we performed a quantitative analysis to assess whether the observed narrow structure could result from the decay cascade via an intermediate nucleon resonance in the $\gamma p \to \pi^0 Res. \to \pi^0\eta p$ process.

Our study considers the effective Lagrangian method at the tree level, incorporating contributions from nucleon resonances $N(1700)3/2^-$ and $N(1710)1/2^+$, which are listed in the PDG review [37] as potential candidates near the energy of interest. The theoretical model includes contributions from s-channel pole diagrams for intermediate resonances as well as t-channel ρ and ω exchanges, s- and u-channel nucleon and Δ pole contributions, and a contact term. Specific intermediate resonance decay processes, such as $N(1440)1/2^+$ and $N(1520)3/2^-$ for $\gamma p \to \pi^0 N(1700)3/2^- \to \pi^0\eta p$, and $N(1535)1/2^-$ for $\gamma p \to \pi^0 N(1710)1/2^+ \to \pi^0\eta p$, are explicitly included.

Theoretical results show that the contribution of the decay cascade $\gamma p \to \pi^0 N(1700)3/2^- \to \pi^0\eta p$ is orders of magnitude smaller than the experimentally extracted narrow structure signal [36], making $N(1700)3/2^-$ an unlikely candidate. For $N(1710)1/2^+$, although a qualitative description of the invariant mass distribution of the narrow structure is obtained, the theoretical cross-section width is significantly larger than in the experimental results. Thus, $N(1710)1/2^+$ cannot adequately explain the observed narrow structure either. These findings indicate that the decay cascade via intermediate nucleon resonances, whether $N(1700)3/2^-$ or $N(1710)1/2^+$, cannot account for the narrow structure observed in the ηp invariant mass distributions of the $\gamma p \to \pi^0\eta p$ reaction.

In conclusion, the observed narrow structure in ηp invariant mass distributions is unlikely to arise from decay cascades involving intermediate resonances. Among the candidates investigated, $N(1710)1/2^+$ contributes more than $N(1700)3/2^-$ but this contribution is insufficient to explain the narrow structure. This result supports the understanding that the $\gamma p \to \pi^0\eta p$ reaction is predominantly governed by decay cascades via the $\Delta(1232)$ resonance, as suggested in previous studies.

ACKNOWLEDGMENTS

The authors thank Fei Huang for useful discussions.

References

[1] N. Isgur and G. Karl, Phys. Rev. D **18**, 4187 (1978)
[2] S. Capstick and N. Isgur, Phys. Rev. D **34**, 2809 (1986)
[3] U. Löring, B. C. Metsch, and H. R. Petry, Eur. Phys. J. A **10**, 395 (2001)
[4] R. G. Edwards, N. Mathur, D. G. Richards *et al.* (Hadron Spectrum Collaboration), Phys. Rev. D **87**, 054506 (2013)
[5] G. P. Engel, C. B. Lang, D. Mohler *et al.* (BGR [Bern-Graz-Regensburg] Collaboration), Phys. Rev. D **87**, 074504 (2013)
[6] R. Koniuk and N. Isgur, Phys. Rev. Lett. **44**, 845 (1980)
[7] S. H. Kim, A. Hosaka, and H. C. Kim, Phys. Rev. D **90**, 014021 (2014)
[8] J. He, Phys. Rev. C **89**, 055204 (2014)
[9] X. Y. Wang and J. He, Phys. Rev. D **95**, 094005 (2017)
[10] Y. Zhang, A. C. Wang, N. C. Wei *et al.*, Phys. Rev. D **103**, 094036 (2021)
[11] R. Bradford *et al.* (CLAS Collaboration), Phys. Rev. C **73**, 035202 (2006)
[12] T. Mart, Phys. Rev. D **100**, 056008 (2019)
[13] N. Zachariou *et al.* (CLAS Collaboration), Phys. Lett. B **827**, 136985 (2022)
[14] N. Zachariou *et al.* (CLAS Collaboration), Phys. Lett. B **808**, 135662 (2020)
[15] N. C. Wei, A. C. Wang, F. Huang *et al.*, Phys. Rev. D **105**, 094017 (2022)
[16] A. C. Wang, N. C. Wei, and F. Huang, Phys. Rev. D **105**, 034017 (2022)
[17] N. C. Wei, A. C. Wang, F. Huang *et al.*, Phys. Rev. C **101**, 014003 (2020)
[18] A. V. Anisovich *et al.* (CLAS Collaboration), Phys. Lett. B **771**, 142 (2017)
[19] K. Moriya *et al.* (CLAS Collaboration), Phys. Rev. C **88**, 045201 (2013)
[20] A. C. Wang, W. L. Wang, and F. Huang, Phys. Rev. D **101**, 074025 (2020)
[21] Y. Zhang and F. Huang, Phys. Rev. C **103**, 025207 (2021)

[22] N. C. Wei, Y. Zhang, F. Huang *et al*., Phys. Rev. D **103**, 034007 (2021)
[23] N. C. Wei, F. Huang, K. Nakayama *et al*., Phys. Rev. D **100**, 114026 (2019)
[24] M. Döring, E. Oset, and D. Strottman, Phys. Rev. C **73**, 045209 (2006)
[25] J. Ajaka, Y. Assafiri, O. Bartalini *et al*., Phys. Rev. Lett. **100**, 052003 (2008)
[26] V. L. Kashevarov *et al*. (Crystal Ball at MAMI, TAPS and A2 Collaborations), Eur. Phys. J. A **42**, 141 (2009)
[27] A. Fix, V. L. Kashevarov, and M. Ostrick, Nucl. Phys. A **909**, 1 (2013)
[28] M. Döring, E. Oset, and U. G. Meißner, Eur. Phys. J. A **46**, 315 (2010)
[29] V. Sokhoyan *et al*. (A2 Collaboration), Phys. Lett. B **802**, 135243 (2020)
[30] A. Fix, Eur. Phys. J. A **58**, 109 (2022)
[31] A. Martinez Torres, K. P. Khemchandani, and E. Oset, Phys. Rev. C **107**, 025202 (2023)
[32] T. Ishikawa, H. Fujimura, H. Fukasawa *et al*, Phys. Rev. C **104**, L052201 (2021)
[33] V. Sokhoyan *et al*. (A2 Collaboration), Phys. Rev. C **97**, 055212 (2018)
[34] V. R. Debastiani, S. Sakai, and E. Oset, Phys. Rev. C **96**, 025201 (2017)
[35] V. Kuznetsov *et al*, JETP Lett. **106**, 693 (2017)
[36] V. Metag *et al*. (CBELSA/TAPS Collaboration), Eur. Phys. J. A **57**, 325 (2021)
[37] R. L. Workman *et al*. (Particle Data Group), PTEP **2022**, 083C01 (2022)
[38] L. Roca, E. Oset, and J. Singh, Phys. Rev. D **72**, 014002 (2005)
[39] J. J. Xie, G. Li, and X. H. Liu, Chin. Phys. C **44**, 114104 (2020)
[40] K. Wang and B. C. Liu, Phys. Rev. C **107**, 025203 (2023)
[41] A. C. Wang, W. L. Wang, F. Huang *et al*., Phys. Rev. C **96**, 035206 (2017)
[42] D. Rönchen, M. Döring, F. Huang *et al*., Eur. Phys. J. A **49**, 44 (2013)
[43] A. C. Wang, W. L. Wang, and F. Huang, Phys. Rev. C **98**, 045209 (2018)
[44] H. Haberzettl, Phys. Rev. C **56**, 2041 (1997)
[45] H. Haberzettl, K. Nakayama, and S. Krewald, Phys. Rev. C **74**, 045202 (2006)